



European Space Research
and Technology Centre
Keplerlaan 1
2201 AZ Noordwijk
The Netherlands
Tel. (31) 71 5656565
Fax (31) 71 5656040
www.esa.int

DOCUMENT

EChO science beyond exoplanets

Document Leads: P. Drossart, G. Micela, B. Swinyard, I. Snellen and P. Hartogh with contributions from J.C. Morales, J.P. Beaulieu and V. Coudé du Foresto

Prepared by P. Drossart, G. Micela, B. Swinyard, I. Snellen, P. Hartogh with contributions from J.C. Morales, J.P. Beaulieu, V. Coudé du Foresto; and the EChO Study Science Team
Reference **EChO-PhaseA-SRE-SA-005**
Issue 1
Revision 0
Date of Issue 13th December, 2013
Status
Document Type
Distribution

European Space Agency
Agence spatiale européenne



APPROVAL

Title ECHO science beyond exoplanets	
Issue 1.0	Revision 0
Author Pierre Drossart G. Micela, B. Swinyard, I. Snellen, P. Hartogh, with contributions from J.C. Morales, J.P. Beaulieu, V. Coudé du Foresto, and the EChO Study Science Team	Date 13/12/2013
Approved by	Date

CHANGE LOG

Reason for change	Issue	Revision	Date

CHANGE RECORD

Issue	Revision		
Reason for change	Date	Pages	Paragraph(s)



Table of contents:

1	Introduction	4
2	Observations of Young Stellar Objects	4
3	Direct observations of Solar System objects with EChO	7
3.1	Interest for solar system observations	7
3.2	Method of observation:.....	8
3.3	Wavelength coverage.....	8
4	Stellar occultations on Solar System Kuiper Belt Objects	9
4.1	Science objectives:	9
5	Planetary seismology	10
5.1	Observability	10
5.2	Science objectives	10
5.3	Observation strategy:.....	10
5.4	Requirements:	11
5.5	Observation strategy:.....	11
6	Brown dwarf observations	12
6.1	Science case.....	12
6.2	Brown Dwarf atmosphere models	14
6.3	Radiometric models SNR	15
6.4	Summary and conclusions	18
7	References	19

1 INTRODUCTION

The capabilities of the ECHO Space Observatory, although dedicated for exoplanets characterization, are also well suited to address some important science objectives in astrophysics. Within the lifetime of EChO and using a small proportion of observing time, or with open time observations, a list of science objectives can be obtained, with an outstanding science return, not available from ground-based or space telescopes.

In this document, we describe a selection of science objectives beyond the primary EChO science on exoplanets, addressing specific questions important in several fields of astrophysics, in particular stellar physics and planetology.

2 OBSERVATIONS OF YOUNG STELLAR OBJECTS

Classical T Tauri stars (CTTSs) have not yet dissipated their circumstellar disks and are still contracting towards the main sequence. While in earlier phases the star is completely embedded in its original nebula, and therefore invisible at optical wavelength, during the T Tauri phase the star has emerged in the visible band and the majority of circumstellar material is concentrated in a disk of gas and dust. During this phase the stellar emission is observed to be significantly variable on many time scales, due to accretion and stellar activity. The observed spectrum is the composite of the stellar photospheric emission dominating the optical band; emission due to accretion, which is responsible for a blue continuum and emission lines, among which characteristically prominent and broad hydrogen lines, and of the disk emission which dominates in the IR band. Such characteristics make T Tauri stars very suitable targets for EChO, since their observations may take advantage of its broadband instantaneous spectral coverage, simultaneously probing the time-variable photosphere, accretion, and the disk up to a distance of a few AUs, and all this with good time resolution.

With its unique capabilities, EChO will address several open questions, among which will be:

1. pinpointing the physical mechanisms responsible for variability in CTTSs on several time scales;
2. determining the physical properties of dusty structures causing the observed dips in AA Tau-like stars (stars with variable light curves showing quasi-periodic dips);
3. measuring the size of the inner disk hole, by attempting to use the “reverberation mapping” technique (Bahcall Koslovsky & Salpeter 1972) in a few CTTSs, crucially testing models of disk evolution.

Classical T Tauri stars have complex light curves. High-cadence (from minutes to hours), multi-wavelength data may be used to determine the origin of variability. Identifying and following in time the many physical mechanisms at work (hot spots at the base of dynamic accretion funnels, rotational modulation of the hot and cool photospheric spots, variable extinction, the dynamic evolution of dust and gas at the inner disk) requires obtaining accurate photometry over a broad band. Spectral variations may indicate the relative weight of hot spots (bluest – due to accretion of

free-falling material on the stellar surface) and cool spots (redder – due to “normal” magnetic activity). As estimated in the analysis of activity-related cool spots (G. Micela, TN on Stellar Activity) EChO will be sensitive to spots a few hundreds of degrees cooler or hotter than the unperturbed photosphere, even with small, $< 1\%$, filling factors. Observations should be carried over time-scales comparable with stellar rotational, typical from days to tens of days on the lifetime of such structures. On shorter time-scales of orders of hours it will be possible to explore the lifetime and properties of accretion events.

The broad spectral coverage may permit also to understand how accreting hot spots may affect the disk properties modifying its structure, for example heating the inner edge of the disk at $T > 1500$, the sublimation temperature of the dust. The rapid sublimation of the dust together with the motions of material will produce large structural changes in the emitting area of the inner disk (Flaherty et al. 2013). Similarly, magnetic flares, which will be readily detectable in the blue part of the observed spectra, will likely produce modifications of the inner disk observable in the IR.

Figure 1 shows an example of simultaneous monitoring of a CTTS in NGC2264 observed with CoRoT and Spitzer for more than 30 days. Variations of tenths of a magnitude are frequently seen both in visible and- IR bands. EChO will not produce such long series but may sample the curve on several time scales, with snapshots at days, weeks or months apart, probing at a precision of few hundredths or even more (depending on the stellar magnitude, sampled times and spectral bin) in the entire band.

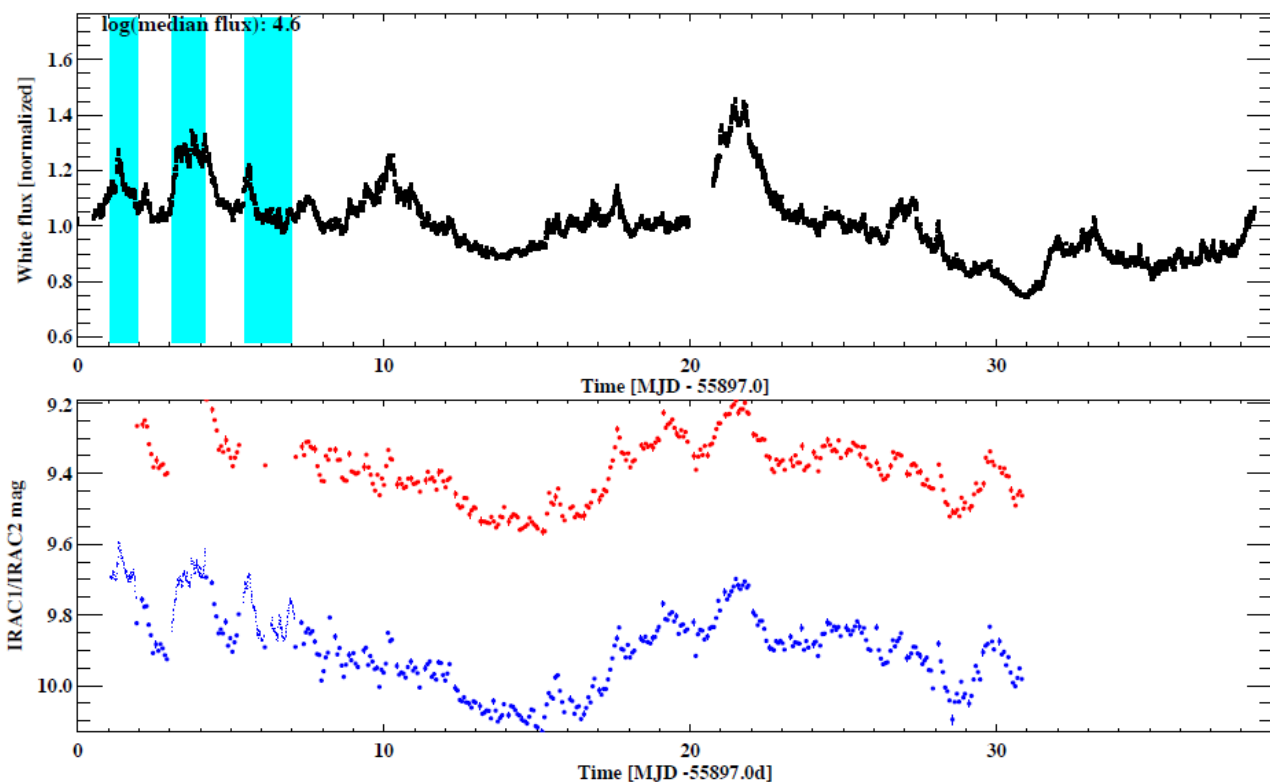


Figure 1: Light curve of a Classical T Tauri Stars in NGC 2264 observed with CoRoT (top panel) and Spitzer (lower panel). Blue shaded areas mark the Spitzer observations made with staring mode to have larger accuracy (courtesy of E. Flaccomio).

Models of accreting pre main sequence stars predict that the inner dusty disk is truncated, because of magnetospheric mechanisms. The presence of an internal wall modifies the spectrum of the star-disk system and produces variability in the IR since the inner disk varies in position and height (Espaillat et al. 2010) and because it may be warped (Bouvier et al. 2003; Romanova et al. 2003, 2009). The truncation of the inner disk has also a role in stopping planet migration toward the central stars. The flux dips in AA Tau-like stars offer a good laboratory to study the structure of the inner disks. These stars have warped disks that quasi-periodically eclipse the stellar photosphere as they orbit their host stars. The wavelength dependence of the variations is a function of the grain size distribution with a peak at wavelength comparable with the typical grain size, which therefore may be derived with EChO observations (see Fig. 2).

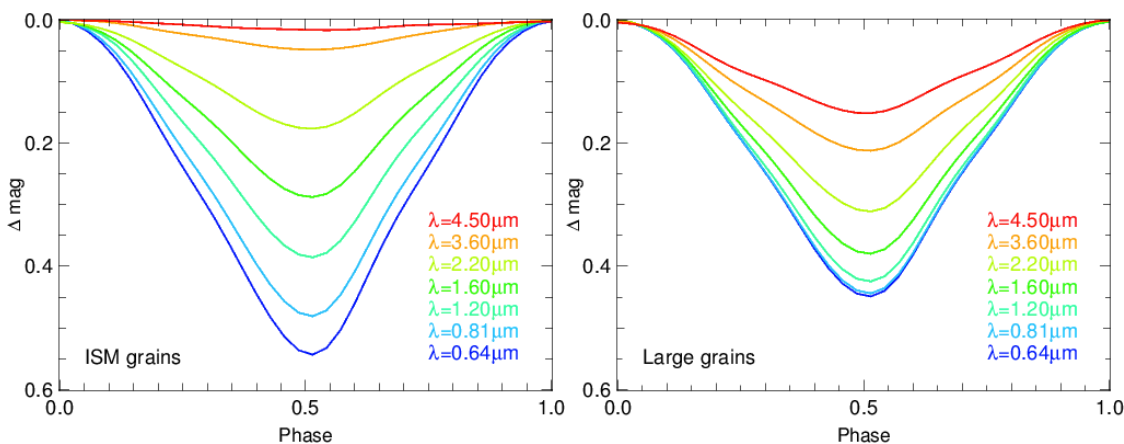


Figure 2: Light curves predicted by a model with a truncated inner disk ($R_{in} = 0.125$ AU) surrounding a T Tauri star ($T_{eff} = 4\,000$ K). Left panel: model with ISM grains (between 0.03 and $1\,\mu\text{m}$). Right panel: model with larger grains (between $10\,\mu\text{m}$ and $1\,\text{mm}$). The wall has the same extinction in the H band in both models.

The AA Tau analysis (described above) will allow us to model flux variations due to extinction and thus constrain the inner disk structure. The Weak-Lined T Tauri stars (YSO without disks, or WTTs) will allow us to observe the wavelength dependent signature of cold magnetic spots, and constrain what fraction of the variability of CTTs can be due to that mechanism. The EChO band includes several accretion indices (the hydrogen line series, K- mid-IR color), which may be used to measure accretion variability. Phase shifts of variations at different wavelengths may allow us to derive the relative longitude of structures on the disk and on the stellar surface giving information on the differential (or locking of) rotation between the star and the inner disk.

Reverberation mapping has been used to map the location of dense clouds in the torus or outflow regions of AGN (Peterson & Wandel 2000). Stellar flares on YSOs may provide an analogous means to directly measure the distance of the inner disk wall from the stellar photosphere by accurately measuring the time delay between the occurrence of photospheric flares, in the optical band, and that of the induced disk flare in the IR, e.g. measuring the delay between times of maximum light. If the inner disk wall has a distance from the stellar photosphere of ~ 0.1 AU, suggested by indirect observations (e.g. SED modelling) the delay will be of only 48 seconds – measurable with EChO. The same targets observed for studying variations on various timescales, are frequently subjected to flare, and therefore suitable for

performing reverberation mapping experiments. A cartoon of the reverberation mapping experiment is shown in fig. 3.

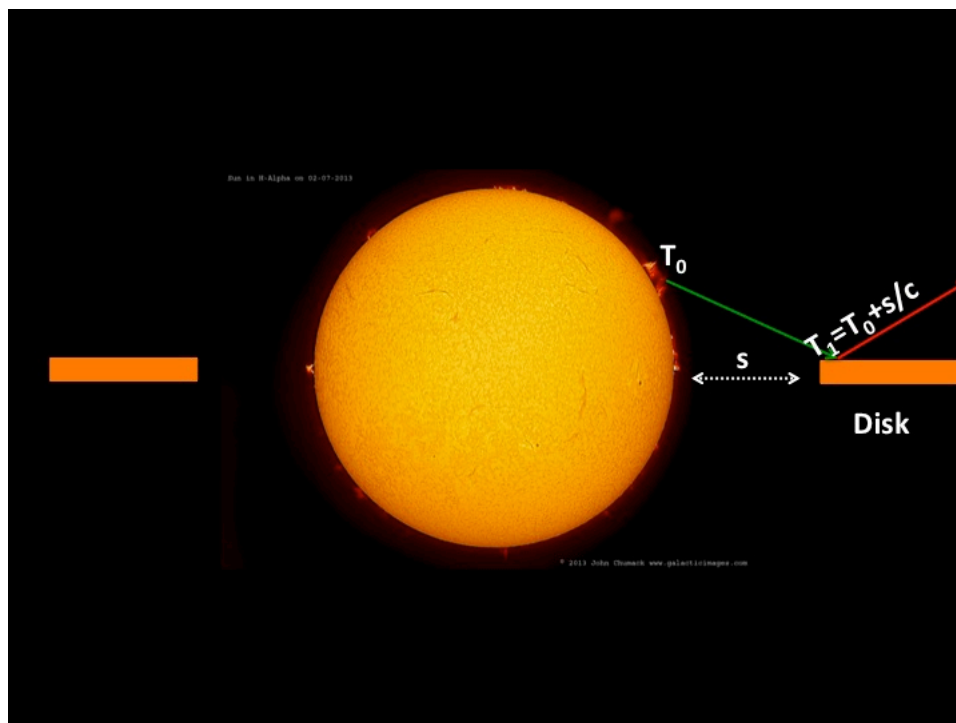


Figure 3: Scheme of the reverberation mapping phenomenon. The central star is a H α solar image (Credit and copyright: John Chumack <http://www.universetoday.com/99823/astrophotos-an-amazing-rush-from-the-sun/>). T_0 is the starting time of the optical flare, s is the distance from the star to the inner disk, T_1 is the starting time of the infrared flare from the disk

3 DIRECT OBSERVATIONS OF SOLAR SYSTEM OBJECTS WITH ECHO

3.1 Interest for solar system observations

The spectra of the Solar System planets and of most of the satellites or small bodies have been extensively studied by dedicated or observatory space missions. Therefore, the primary interest for Solar System observations will reside in the calibration of EChO spectrometer compared to known objects. In terms of outreach, obtaining spectra of many objects from the same spectrometer will also be valuable for textbooks references. Since the observations on target for most of the objects will require a minimum time, it will be valuable to dedicate a portion of time in EChO observations for Solar System objects, to acquire directly their spectra.

3.2 Method of observation:

The slit size on the EChO instrument will be $\sim 2 \times 10$ arcsec with a few spatial elements (3 to 5 depending on the final design) in the “long direction”. This will allow some spatial discrimination on the larger planets as shown in table 1. The wavelength

Target	Diameter	Target	Diameter
Mars	25.1"	Neptune	2.4"
Ceres	0.84"	KBO/Pluto	0.11"
Vesta	0.64"	Io	1.2"
Jupiter	50.1"	Ganymede	1.8"
Saturn	20.1"	Titan	0.8"
Uranus	4.1"	Triton	0.13"

Table 4.2.1 Planetary characteristics (diameter is an average for observations at Earth orbit).

3.3 Wavelength coverage

Table 4.3.1 Table of observables

Object	EChO Band				
	VNIR (0.55-2.5 μm)	SWIR (2.5 – 5 μm)	MWIR1 (5-8 μm)	MWIR2 (8-11 μm)	LWIR (11-16 μm)
Mars	Clouds, Surface, Dust	Too cold	Surface temperature, water vapour, dust	Surface temperature, dust	Surface temperature. Atmospheric temperature (CO_2), dust
Jupiter	Clouds	Deep atmosphere – abundances and cloud layers, plasmasphere (H_3^+ ?, auroral)	Stratospheric temperature (CH_4)	NH_3 , PH_3 convection	Tropospheric temperature, H_2/He CIA. Hydrocarbons?
Satellites	Titan clouds, weather	Io plasmasphere? Titan clouds, weather	Io plasmasphere?		Titan hydrocarbons, nitriles
Saturn	Clouds	Deep atmosphere – abundances and cloud	Stratospheric temperature (CH_4)	PH_3 convection	Tropospheric temperature, H_2/He CIA. Hydrocarbons

		layers, aurora			
Uranus	Clouds	SFA	SFA	SFA	H2/He CIA Seasonal variations
Neptune	Clouds	SFA	SFA	SFA	H2/He CIA, hydrocarbons seasonal variations
Comets	Dust, H2O, NH3	Dust, H2O, CO, CO2, NH3	Dust	Dust	Dust, CO2
Minor, NEOs Asteroids	Surface	Surface, water ice	Surface	Thermal inertia, Surface	Thermal inertia, Surface

4 STELLAR OCCULTATIONS ON SOLAR SYSTEM KUIPER BELT OBJECTS

Planetary occultations (including planets as well as Kuiper Belt objects, Pluto being one of them), observed when a planet is passing in front of a star, will be used to search for atmospheric perturbations during occultation. Ground based observations of occultations by Pluto have allowed the observation of the evolution of planetary atmosphere with time, from regular observations of occultation (e.g. Sicardy et al., 2011).

An occurrence of ~1 event/year for KBO large objects (Pluto, Quaoar, etc.) can be expected. Nevertheless, these occultations are rare, and several limitations are present. The inversion of the light curve during occultation gives a measurement of the refractive index variation with altitude on the planet, itself related to the atmospheric pressure. Observations with spectroscopy gives access to spectral variation of the refractive index, which are expected to provide information on the atmospheric composition. The observations would be very similar to exoplanets occultations, except that a highest repetition time as possible is necessary, with occultation event lasting only for less than a minute.

4.1 Science objectives:

- atmospheric composition (from spectra), structure of the atmosphere
- search for extended dust rings around the objects

Requirements: repetition time for observation lower than 1 sec

Observation strategy: the pointing can be maintained on the star, so there is no specific pointing requirement.

The most obvious observations, similar to the transit observations of exoplanets would be to look at planetary occultations, searching for atmospheric perturbations during occultation.

For Pluto, an occultation by a star brighter than 11th magnitude is expected at most once every two years (in the visible), with better statistics in the infrared (one per year)

For Kuiper Belt Objects and Centaurs, several objects are also passing in front of the Milky Way with occultation occurrence similar to Pluto; Quaoar or Chariklo are good candidates.



The main limitation for EChO observations will be the repetition time: from the ground, the repetition time for occultation observations is better than 1sec. For a repetition time of 30s, only one or two spectra will be recorded, due to the apparent velocity of the object. Only if high repetition rate (1 or a few seconds) are manageable will the observations be valuable.

5 PLANETARY SEISMOLOGY

Planetary interiors can be probed by seismology, which consists in identifying acoustic modes from a continuous long term observation of planets – the coherence of these modes ensures a detection of acoustic modes against a more chaotic variability due to meteorological activity. Observations of global oscillations of Jupiter have been obtained from ground based observations (Gaulme et al, 2011), detecting for the first time an excess power in the power spectrum of time series, and measuring the Jovian fundamental frequency. Planetary oscillations are similar to oscillating stars, as observed for example with Corot (Appourchaux et al., 2008). The method of observations with EChO would consist in observing a planet for the longest continuous time (3 to 7 days, with interruptions for data downlinking of ~2 hours acceptable). In addition to photometric observations, spectroscopic observations would give access to different atmospheric layers, constraining the vertical structure of the oscillations. Normal-mode oscillations would place new constraints on Uranus and Neptune interior, and on the origin and evolution of these planets.

5.1 Observability

Due to the EChO aperture, only Uranus and Neptune are observable (Jupiter and Saturn being too large). There is no theoretical prediction available for the amplitude of the planetary oscillations – Neptune being more active (energy balance larger than Uranus), seems a more favorable candidate than Uranus, as internal convection is assumed to excite internal acoustic waves.

5.2 Science objectives

The search for planetary oscillations will be made through long duration continuous spectral observations in the infrared. The oscillations emerge from the search of characteristic frequencies in the Fourier transform of the photometric temporal variations. Looking at different wavelengths allow to sound at different atmospheric layers, depending on the opacity of the atmosphere.

5.3 Observation strategy:

- Continuous observations: 7 days (with interruption of ~2 hours for data transmission)
- Repetition time 1 min to 90 sec.

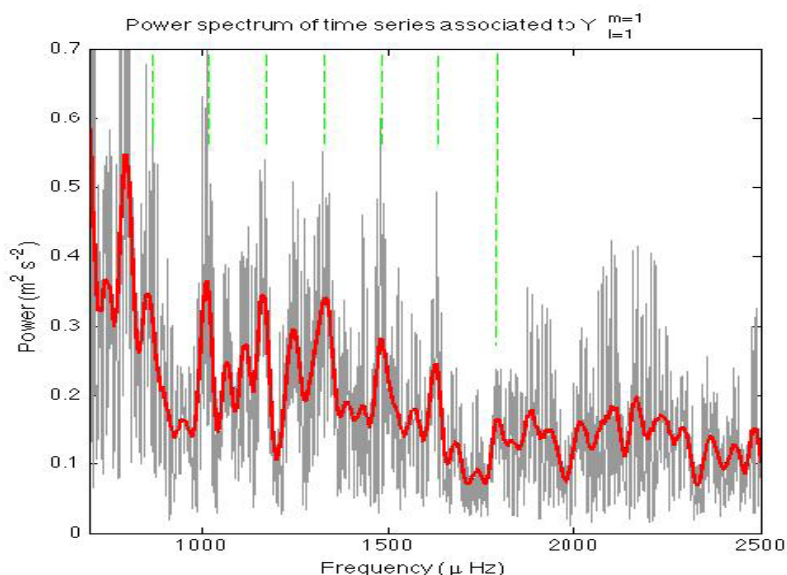


Fig. 4 Power spectrum of Jupiter time series obtained with SYMPA. 7 peaks may be currently attributed with global modes (Gaulme et al. 2011).

5.4 Requirements:

Observation of moving objects must be implemented for these observations. Giant planet seismology, built on the observations of helio and asteroseismology, give access to the interior structure and atmospheric dynamics of these objects. The detection of oscillation modes, even for Jupiter, has proved to be extremely difficult, due to the degeneracy of the modes for a rotating planet, and has only recently been confirmed with a good degree of confidence for Jupiter (Gaulme et al, EPSC conference, 2011 and paper in preparation). Due to the EChO aperture, only Uranus and Neptune are observable. One major science objective would be to search for planetary oscillations through long duration continuous spectral observations in the infrared.

If only one target is feasible, Neptune has the highest priority, as exhibiting more internal activity, for generation of internal waves.

5.5 Observation strategy:

Continuous observations: 7 days (with interruption of ~2 hours for data transmission). Repetition time: 1 min to 90 sec;

Expected flux: peak at 8 micron: $20 \cdot 10^{-14} \text{ W m}^{-2} \text{ Hz}^{-1}$ in 0.12 micron width. Converted to ~2000 electron/sec/pixel.

Observation of moving objects must be implemented for these observations. Typically, the velocities on the sky of Uranus or Neptune are:

Neptune: $< 0.15 \cdot 10^{-2} \text{ arcsec/sec}$

Uranus: $< 0.25 \cdot 10^{-2} \text{ arcsec/sec}$



An ephemeris must be loaded to adapt the drift velocity during the observing period of 1 week.

6 BROWN DWARF OBSERVATIONS

The possibility of building up a homogenous catalogue of Brown dwarfs spanning all the spectral types. By monitoring them over at least one rotation cycle (typically 10 hours), we will characterize their spectral variability typically due to the presence of clouds on their atmosphere. The physics at play in the atmosphere of brown dwarfs is close to the hot Jupiters. Such targets will provide a calibrator to the codes used to decipher the properties of hot Jupiters.

A fraction of the time on board EChO will be dedicated to additional science. The scheduling technote (ECHO-TN-0001-CNES) has shown that there will be a number of gaps, with durations in the range 1-10 hours to observe targets that are not part of the EChO core science. A possibility is to use the gaps of the EChO schedule to build up a homogenous catalogue of spectra of brown dwarfs. A secondary goal is to characterize the spectral variability of brown dwarfs by observing them over at least one rotation period. Several results suggest that this variability may be due to inhomogeneous clouds in the atmosphere of brown dwarfs modulated over one rotation period. In contrast, with hot Jupiters, sharing similar physical conditions in their atmosphere, we only have specific snapshots at the time of transits and occultations.

Simulations using the Radiometric Model (October 2013 version) show that EChO will provide the spectra of brown dwarfs with enough SNR to characterize this variability up to magnitude $K \sim 15$ with a spectral resolution $R=300$ ($\lambda \leq 5 \mu\text{m}$). The brown dwarfs to be observed will need to have a star less than 20 arcsec away in order for the FGS. Given the ongoing large surveys hunting for nearby brown dwarfs, we hope to have such targets for 2024

6.1 Science case

Burgasser (2009) gives an excellent review about the similarities and differences between Brown dwarfs (hereafter BDs) and planets, and what they could teach us. BDs share common characteristics with low-mass M-dwarf stars and with the atmospheres of hot exoplanets. The temperature of the photosphere of the coolest BDs overlaps significantly with the hottest exoplanet atmospheres. However, there are also some differences, such as formation mechanism (and therefore likely different chemical composition), evolutionary effects, processes associated with external driving sources and the higher photospheric gas pressure. BDs are fascinating objects in their own right, being the bridge between planets and stars, but they offer a unique laboratory to analyze the properties of giant planet atmospheres. A systematic and detailed study of condensate cloud formation and non equilibrium chemistry done on BD is an excellent ingredient to understand the same physical process in the hot exoplanet atmospheres.

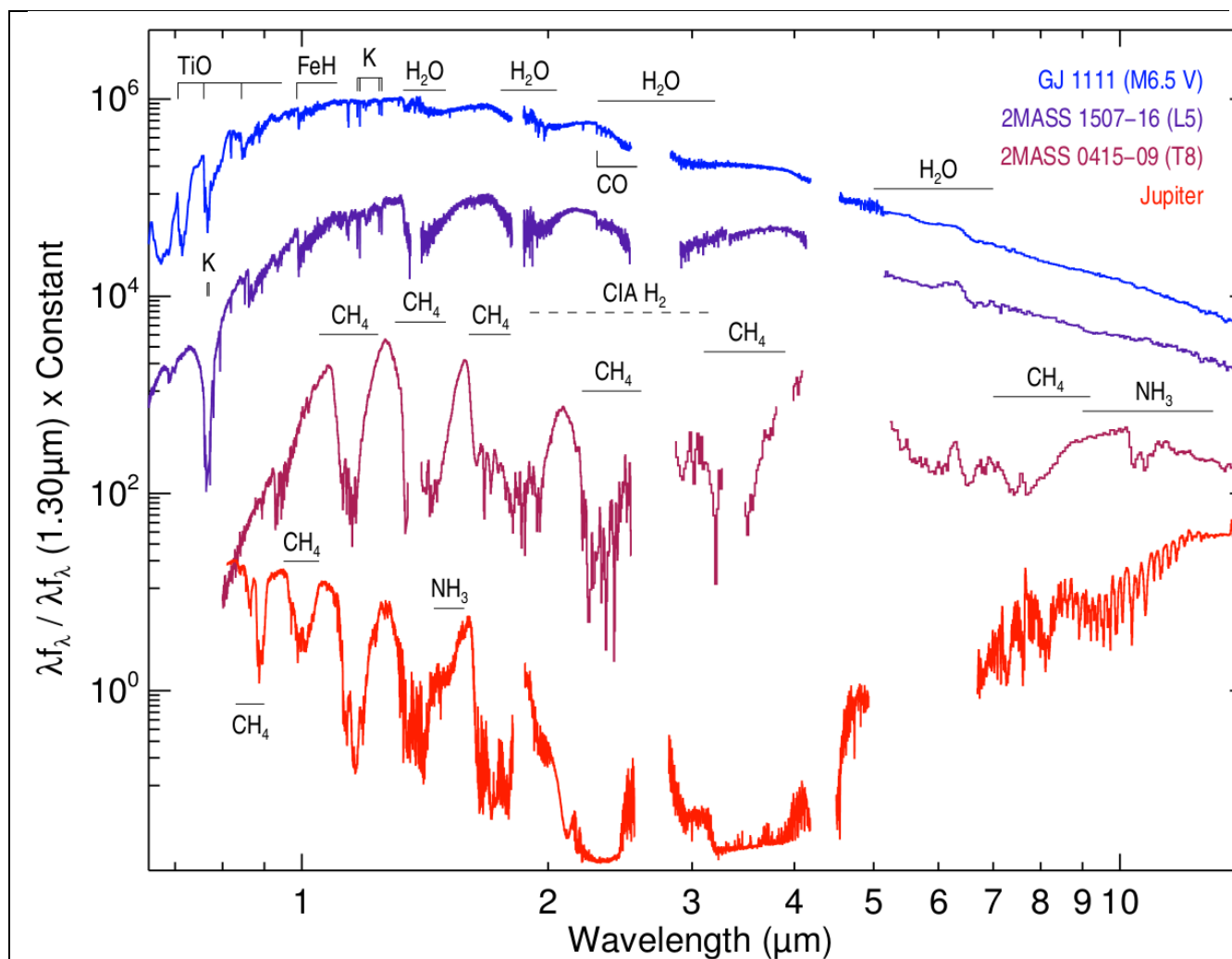


Figure 5: We compare the spectra of a M6.5, L5, T8 and Jupiter over the spectral range 0.5 to 11 microns. The main atomic molecular features for the different spectral types are indicated (From Burgasser 2009).

Kirkpatrick (2005) analyzes in depth the spectral properties of BDs. This review shows that the spectral classification of these objects depends on the wavelength of observation. In particular, the infrared spectrum predicts almost the same effective temperature of about 1500 K from mid-L to mid-T dwarfs. On the other hand, many direct imaging giant exoplanets with spectral types similar to BDs have been found to be redder and fainter than expected. The presence of regions with different effective temperatures or clouds has been proposed as an explanation of these differences.

In a recent paper, Apai et al. (2013) show the spectroscopic follow-up of two BDs. They detect peak-to-peak variations of up to ~27% on the *J* and *H* bands (similar results were also found by Radigan et al. 2012). They conclude that they can explain this spectrophotometric variations assuming the presence of spots or clouds on the atmosphere with a temperature difference of about ~300 K and a filling factor of 20-30%.

We propose to use EChO to observe a sample of brown dwarf spanning all the spectral range, and to characterize their spectroscopic variability. Note that there are not transiting brown dwarfs. We are going to take emission spectra of them (assuming that the target chosen have a star in the EChO field of view to use the FGS).

The main challenge is to spectroscopically characterize brown dwarfs is their intrinsic faintness. The dwarfarchives.org database lists a total of 918 and 355 L- and T-type brown dwarfs respectively. Figure 6 shows the K_s magnitude distribution of these targets. Magnitude ranges from 10 to 21 mag, with a peak at ~ 14 mag for L dwarfs, and at ~ 15 for T dwarfs. Although, this magnitude is fainter than the requirements of the EChO mission for the the detection of exoplanets, it may still be enough to observe the spectra of brown dwarfs with sufficient SNR.

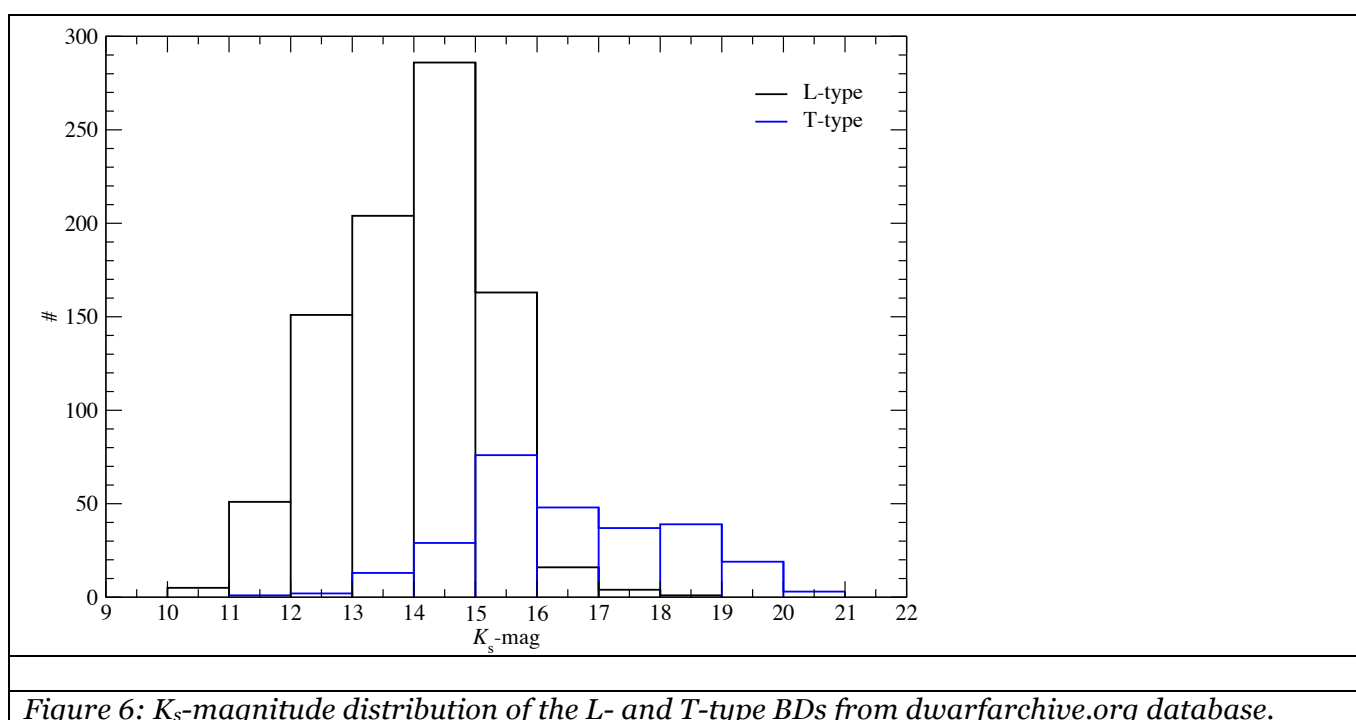


Figure 6: K_s -magnitude distribution of the L- and T-type BDs from dwarfarchive.org database.

6.2 Brown Dwarf atmosphere models

In order to estimate the expected SNR of brown dwarf spectra observed with EChO, the stellar emission was modeled using the spectral energy distributions (SEDs) provided by Phoenix models (BT-Settl. stellar atmosphere models : Allard et al. 2011) with a surface gravity of 4.5 and solar metallicity. The empirical effective temperature-spectral type relations of Golimowski et al. 2004 were used to compute the effective temperature at each spectral type (listed in Table 1) and to interpolate the grid of theoretical SEDs.

	Spectral type	T_{eff} (K)	Spectral type	T_{eff} (K)	
	Lo	2300	To	1450	
	L1	2200	T1	1450	

L2	2080	T2	1440
L3	1950	T3	1400
L4	1820	T4	1330
L5	1700	T5	1220
L6	1600	T6	1060
L7	1520	T7	890
L8	1480	T8	750
L9	1460	T9	700

Table 1: Effective temperature for each spectral subtype according to the empirical relation by Golimowski et al. 2004). Predicted T_{eff} for T0 and T1 spectral types do only differ by few K, therefore the same temperature is assumed.

Figure 7 shows the theoretical SEDs for some representative brown dwarf (BD) subtypes. The spectrum is highly dominated by molecular and atomic lines. There are significant differences between different spectral subtypes for wavelengths up to 10 μm . Near-IR H_2O bands strengthen from L0 to T9, and CH_4 absorption appears at mid-T spectral types.

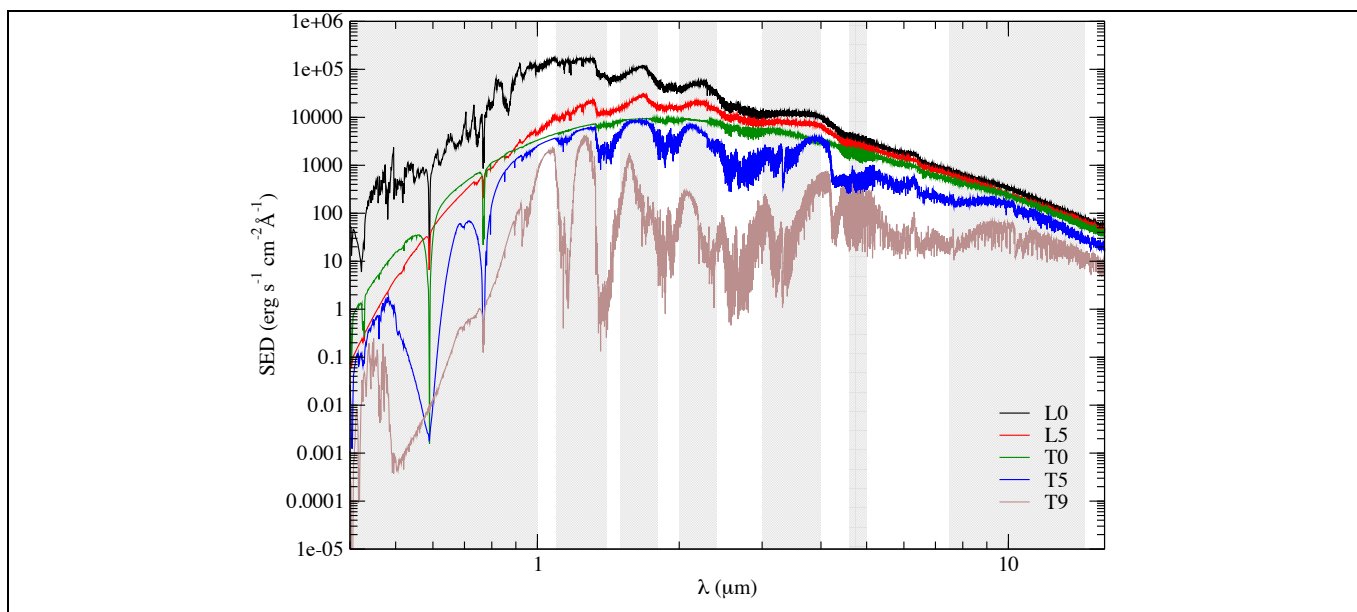


Figure 7: Theoretical SEDs of BDs from Allard et al. (2011). Earth atmosphere infrared windows are highlighted in grey.

6.3 Radiometric models SNR

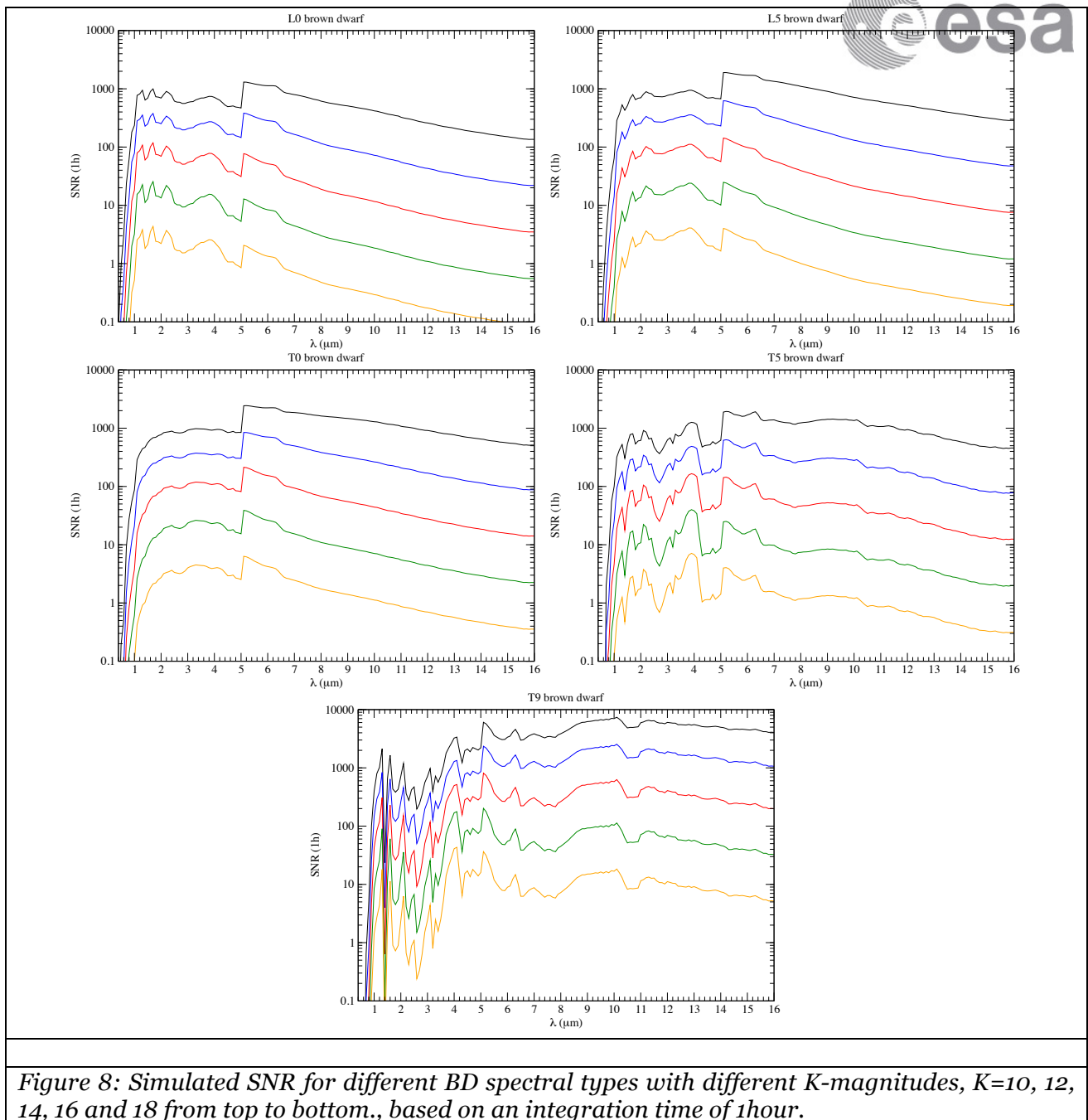
We estimated the signal to noise ratio for each spectral type of BDs using the Radiometric Model (version “Rad Mod – Oct2013”). This model computes the SNR of the stellar signal as a function of the wavelength for the set of SED models described in the previous section. Standard values for the



total throughput (10% and 23% for 0.4-2 μm and for 2-16 μm , respectively) and a spectral resolution of $R=300$ (0.4-5 μm) and $R=30$ (5-16 μm) were assumed, although a resolving power between 50-100 is expected for exoplanets on the NIR band.

We simulated the cases of L0, L5, T0, T5, and T9 spectral type BD with K -magnitude ranging from 10 to 18 mag. The radii of BDs were set to about one Jupiter radius (0.1 solar radius) for all cases in order to compute the distance for each magnitude. We fixed the exposure time to 1h per observation.

Typical photometric variability of brown dwarfs is around 10% to 30% depending of the wavelength. Therefore we estimated that with a $\text{SNR} \sim 30$ on the BD spectra it will be enough to detect variability of about 10% of the flux with 3σ confidence. Figure 8 shows the SNR as a function of wavelength for the spectral types simulated. We conclude that, in the NIR and MIR regions, the required SNR can be achieved for BD up to magnitudes around $K \sim 15$ mag. In this simulation, we did not take into account possible deviations due to the pointing stability on faint BDs.



In order to estimate the effect of clouds or temperature spots on BD, we also simulated the case of a BD composed by two different spectral subtypes, 80% of the surface due to a L5 BD and 20% due to a To BD, with a temperature difference of 250 K and a magnitude of $K=14$ (average value for L5 BD in the dwarfarchive.org database). This would be equivalent to a L5 BD with a spot covering 20% of its surface. Figure 9 shows the spectrum of the spotted BD normalized to the immaculate spectrum of a L5 BD. Shaded area correspond to the noise simulated using the Radiometric Model. This figure shows that the SNR in the region between 1 and 7 μm , where the changes of the molecular bands are more significant, will be enough to detect the variability due to spots. In the visual bands, where the emission of BD is smaller, or in the far infrared wavelengths, where the effect of spots is

smaller, the variability will not be detected. In the case of clouds of H₂O or CH₄, the variability on their characteristic spectral bands can even be larger, and therefore easier to detect.

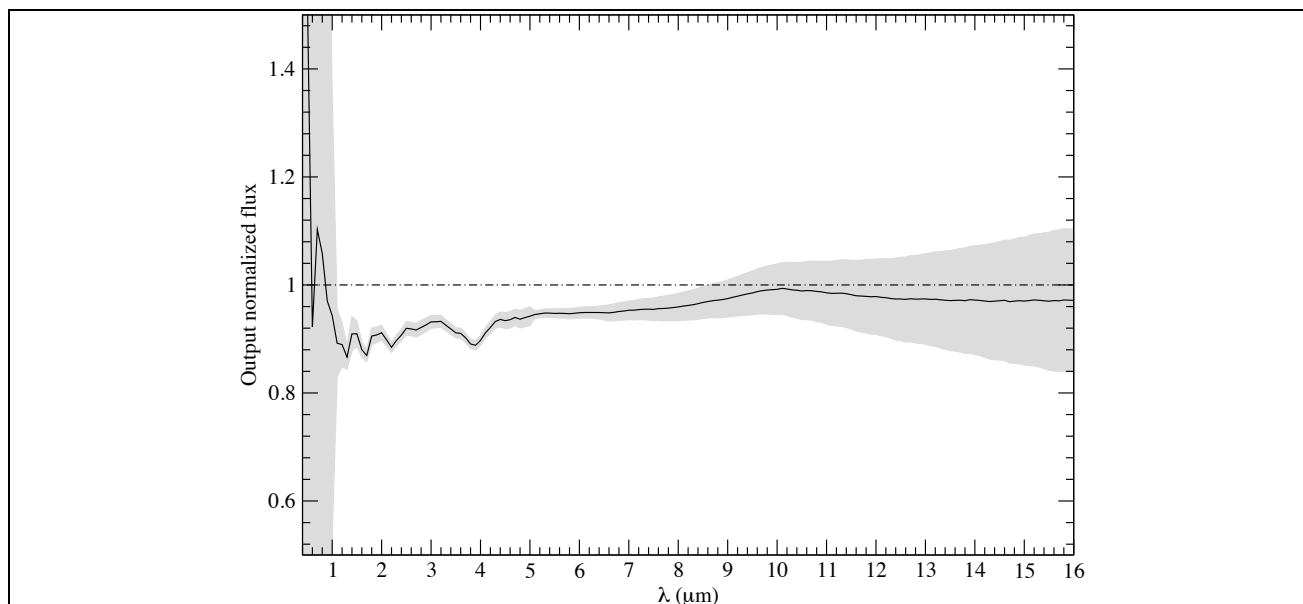


Figure 9: Simulation of the observation of a L5 BD with a cool spot filling 20% of its surface with a temperature 250 K cooler. K-magnitude of the object is fixed to 14 mag. The spectrum is normalized to the L5 immaculate spectra. Shaded region corresponds to the expected SNR computed with the Radiometric Model of EChO

EChO technote on scheduling (ECHO-TN-0001-CNES), show that some of the gaps between observations are longer than 10h. We suggest using these gaps to observe BDs in the L-T transition. The typical rotation periods of evolved BD are below 1 day, with mean values of about 15h (Scholz & Eislöffel 2005). We suggest to perform follow up during at least one rotation cycle of variable brown dwarfs to characterize their spectral variability, that we will be able to compare with hot Jupiters of similar temperature.

A list of BD targets that can be observed with EChO is given in the appendix (give section number of appendix). The selection of these BDs is based on the presence of a bright companion within 20 arcsec that can be used as guiding star for FGS.

6.4 Summary and conclusions

Recent results have revealed that the spectroscopic variability of brown dwarfs of about 20-30% can be explained by the presence of clouds on the atmosphere. This can also explain the problems of classification using the NIR spectra or the sub-luminosity of some giant planets with similar spectral profiles.

We propose to have a sample of brown dwarf to be observed as part of the additional science. We would use the gaps in the scheduling of the exoplanet observations to do snapshot observations of



brown dwarfs of a large variety of spectral types, and to monitor the spectroscopic variability of a subset. EChO will provide sufficient SNR to provide an unprecedented catalogue of brown dwarf spectra covering the range 0.5-11 microns at a resolution $R=300$ (up to 5 microns), with good S/N in 1h exposures. Observing brown dwarf with EChO will be a key ingredient in understanding the variability of hot Jupiter with similar atmospheric properties.

A list of brown dwarfs with close companions has been obtained, with a statistics of 38 known observable objects in the category of L-type and 15 in the category of T-type brown dwarfs

7 REFERENCES

Allard et al. 2011. Model Atmospheres From Very Low Mass Stars to Brown Dwarfs. ASPC, 448, 91

Apai et al. 2013. HST Spectral Mapping of L/T Transition Brown Dwarfs Reveals Cloud Thickness Variations. The Astrophysical Journal, Volume 768, Issue 2.

Appourchaux et al., 2008. CoRoT sounds the stars: p-mode parameters of Sun-like oscillations on HD 49933. Astronomy and Astrophysics, Volume 488, Issue 2, 2008, pp.705-714

Bahcall, John N., Kozlovsky, Ben-Zion, Salpeter, E. E. On the Time Dependence of Emission-Line Strengths from a Photoionized Nebula. Astrophysical Journal, vol. 171, p.467

Bouvier et al. 2003. Eclipses by circumstellar material in the T Tauri star AA Tau. II. Evidence for non-stationary magnetospheric accretion. Astronomy and Astrophysics, v.409, p.169-192

Burgasser et al., 2009. Optical and Near-Infrared Spectroscopy of the L Subdwarf SDSS J125637.13-022452.4. The Astrophysical Journal, Volume 697, Issue 1, pp. 148-159

Espaillet et al. 2010. Unveiling the Structure of Pre-transitional Disks. The Astrophysical Journal, Volume 717, Issue 1, pp. 441-457

Flaherty et al. 2013. Kinks and Dents in Protoplanetary Disks: Rapid Infrared Variability as Evidence for Large Structural Perturbations. Astronomical Journal, Volume 145, Issue 3, article id. 66, 23

Gaulme et al, 2011. Detection of Jovian seismic waves: a new probe of its interior structure. Astronomy & Astrophysics, Volume 531, id.A104,

Golimowski et al. 2004. L' and M' Photometry of Ultracool Dwarfs. The Astronomical Journal, Volume 127, Issue 6, pp. 3516-3536

Kirkpatrick, J.D. 2005. New Spectral Types L and T. Annual Review of Astronomy & Astrophysics, vol. 43, Issue 1, pp.195-245

Peterson, B.M. and Wandel, A. 2000. Evidence for Supermassive Black Holes in Active Galactic Nuclei from Emission-Line Reverberation. The Astrophysical Journal, Volume 540, Issue 1, pp. L13-L16

Romanova et al. 2009. Launching of conical winds and axial jets from the disc-magnetosphere boundary: axisymmetric and 3D simulations. Monthly Notices of the Royal Astronomical Society, Volume 399, Issue 4, pp. 1802-1828



Radigan et al. 2012. Large-amplitude Variations of an L/T Transition Brown Dwarf: Multi-wavelength Observations of Patchy, High-contrast Cloud Features. The Astrophysical Journal, Volume 750, Issue 2, article id. 105.

Romanova et al. 2003. Magnetohydrodynamic Simulations of Accretion onto a Star in the ``Propeller" Regime. The Astrophysical Journal, Volume 588, Issue 1, pp. 400-407.

Scholz A. & Eislöffel J., 2005, Rotation and variability of very low mass stars and brown dwarfs near ϵ Ori, Astronomy & Astrophysics, 429, pp. 1007-1023.

Sicardy et al, 2011 A Pluto-like radius and a high albedo for the dwarf planet Eris from an occultation. Nature, Volume 478, Issue 7370, pp. 493-496